

## Variation of Emission Yield of X-rays from Crystals with Diffraction Condition of Exciting Electrons

BY SHIZUO MIYAKE, KAZUNOBU HAYAKAWA AND ROKURO MIIDA

*Institute for Solid State Physics, University of Tokyo, Azabu, Minato-ku, Tokyo, Japan*

(Received 10 June 1967)

The X-ray intensity of Zn  $K\alpha$  radiation emitted from clean cleavage surfaces (110) of zincblende crystals excited by fast electrons, which impinge on the surfaces in the same way as in ordinary electron diffraction experiments, was measured under various diffraction conditions of exciting electrons. The electron energy was about 30 keV. It was found that the X-ray intensity decreases at Bragg conditions by about 10–20%, in an asymmetric way with respect to the glancing angle of the electrons. Some of features of such an anomaly in X-ray intensity have been discussed on the basis of a two-wave dynamical theory of electron diffraction taking account of the phenomenological absorption.

### Introduction

The dynamical theory of X-ray diffraction was first presented by Darwin (1914), and was subsequently formulated independently by Ewald (1917) in a more general form. The dynamical theory for electron waves was given by Bethe (1928). Although earlier applications of these theories were mostly concerned with characteristics in free space of beams diffracted by perfect crystals, such as the refraction effect, the line profiles of reflexions, the integrated intensity and the intensity anomaly due to the dynamical effect, the dynamical theory is essentially a theory which can deal with the spatial distribution of the wave field within a crystal under a given diffraction condition. It is largely due to this feature that the dynamical theory has recently become increasingly important in relation to various practical problems such as those in electron microscopy and X-ray diffraction topography.

Besides the usual coherent or elastic scattering, there are many kinds of interaction effect between the crystal and the incident wave. In the case of X-rays there are photoelectric absorption, the emission of fluorescent X-rays, and Compton and thermal X-ray scattering. In the case of electrons there are inelastic and thermal scattering, and the excitation of characteristic X-rays as well as continuous X-rays. With thermal neutrons there may be some nuclear reaction. Any of these interactions, however, should generally depend on the distribution of the primary wave field formed within the crystal, and hence on the diffraction condition of the incident beam. Near a Bragg condition in particular, some anomalous change is expected to take place in the cross section of the interaction concerned.

A neutron diffraction study on calcite by Knowles (1956), done according to a suggestion of Ewald, was the first in detecting such an anomalous behaviour of the interaction cross-section. In this experiment the intensity of  $\gamma$ -rays emitted from calcium nuclei was measured, and an anomalous change was observed in

the  $\gamma$ -ray emission yield at the Bragg condition of neutron waves.

As to X-ray diffraction experiments, Batterman (1962, 1964) observed a similar effect on the emission of  $K$  fluorescent X-rays from single crystals of germanium excited by Mo  $K\alpha$  radiation, and Annaka, Kikuta & Kohra (1966) observed such an effect on the modified X-ray scattering, including both Compton and thermal scatterings, using silicon and germanium crystals as samples, with Ag  $K\alpha$  and Mo  $K\alpha$ . The experiments by Batterman and by Annaka *et al.* were done under the conditions of the so-called Bragg case (reflexion case), while the condition in Knowles's neutron experiment corresponded to the Laue case (transmission case). Recently, Annaka (1967) studied the fluorescent X-rays from germanium crystals under the conditions of the Laue case.

Concerning the characteristic X-rays excited by fast electrons, Hirsch, Howie & Whelan (1962) have considered theoretically the dependence of their intensity on the diffraction condition of exciting electrons for a thin crystal. In conformity with their theory, Duncumb (1962) observed an enhanced X-ray emission from a thin gold film at intense parts of extinction contours in electron-micrographs. Very recently, Hall (1966) made a more detailed study of the similar effect on

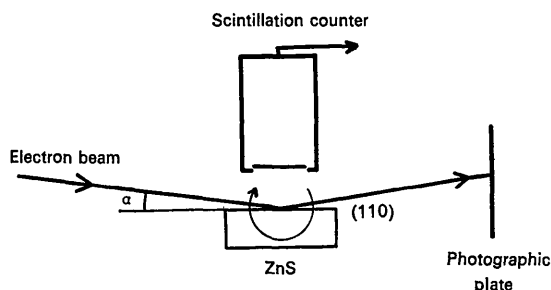


Fig. 1. Schematic diagram of experimental setting.

nickel and germanium films by use of a modified electron microscope provided with a simple X-ray spectrometer and a scintillation counter, and obtained a qualitative agreement with the theory.

The present study also deals with the dependence of the characteristic X-ray emission from a single crystal on the diffraction condition of exciting electrons, and hence has a common purpose with Hall's work. However, the present experiment consists in detecting the Zn  $K\alpha$  radiation emitted from clean cleavage surfaces (110) of thick zincblende (ZnS) crystals, and therefore the diffraction condition of electrons concerned is the Bragg case, in contrast with the case in the studies of Duncumb and Hall. This paper reports preliminary experimental results and some theoretical considerations.\*

### Experimental

The apparatus used is a combination of an electron diffraction camera of ordinary type and an X-ray scintillation counter. Fig. 1 shows schematically the experimental setting adopted. The distance between the sample surface and the window of the counter was about 30 mm. The window of the scintillation counter, which is 15 mm in diameter, is covered with a thin beryllium plate, by which the electrons scattered by the sample are prevented from entering the counter. A copper foil of 20  $\mu$  thickness and several sheets of aluminum foil were inserted between the sample and the counter. The aluminum foils were used mainly for suppressing appropriately the maximum count of X-ray photons. The window of the pulse height analyser was usually 5V in breadth and the base line was set so as to select the Zn  $K\alpha$  radiation. The copper foil inserted cut down Zn  $K\beta$ , and at the same time reduced the continuous X-rays forming the background in the spectral range which was covered.

\* A short report by the present authors has been published elsewhere (Miyake, Hayakawa & Miida, 1966).

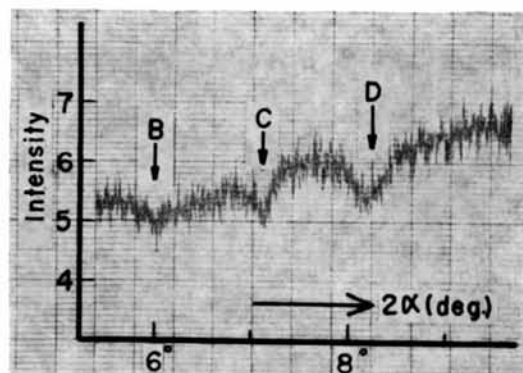


Fig. 3. Intensity variation of emitted X-rays against the scattering angle,  $2\alpha$ , of electrons (30 keV) covering the conditions B, C, and D, for the same crystal azimuth as in Fig. 2. The intensity curve begins, in its measurement, from the right side; the same applies to Figs. 4, 5 and 6.

X-rays caught by the counting system contain both the continuous X-rays and the Zn  $K\alpha$  radiation due to the ionization of K shells of zinc atoms. The Zn  $K$  radiation may be excited not only by electrons with the primary energy, but also by inelastically scattered electrons accompanied by energy losses so long as their energies remain higher than the value corresponding to the Zn  $K$  absorption edge, namely 9.7 keV. The intensity change of characteristic X-rays with the diffraction condition of exciting electrons is expected to take place only with respect to the primary ionization process, while those excited by inelastically scattered electrons will merely result in the formation of a high background. The continuous X-rays also contribute to the background with an intensity which is the more appreciable the higher the electron energy.

For observing the anticipated anomaly of X-ray emission, therefore, it should be profitable to choose the energy of incident electrons at a value not too much exceeding 9.7 keV. There was, however, a necessary compromise because of the requirement that electron diffraction patterns should be observable at the same time, in order to set purposely in advance, or know exactly, the diffraction condition of electrons in each case. Because the pattern observation tends to become unstable when the energy of incident electrons is too low, the electron energy adopted was about 30 keV. The number of X-ray photons counted was usually of the order of  $1 \sim 2 \times 10^3 \text{ sec}^{-1}$ .

The X-ray intensity was measured as a function of the glancing angle,  $\alpha$ , of the electrons incident on the crystal surface, at a fixed azimuth. The angle  $\alpha$  was continuously changed by rotating the crystal about the axis which is perpendicular to the incident beam and lying on the crystal surface, with the rotating velocity  $5' \text{ min}^{-1}$  to  $30' \text{ min}^{-1}$ .

An electron diffraction pattern containing a number of diffraction spots and Kikuchi lines and bands gives an indication of the electron diffraction condition in each case. Fig. 2, for example, is a diffraction photograph for a crystal azimuth deviating about  $5^\circ$  from the  $[\bar{1}12]$  zone axis. The spot  $S$  corresponds to the specular reflexion, and the glancing angle,  $\alpha$ , can be given from its position. The position of  $S$  relative to a Kikuchi line gives a knowledge of the electron diffraction condition with respect to the lattice plane concerned, and the crystal azimuth can also be judged from the Kikuchi pattern.

With the rotation of the crystal the spot  $S$  moves vertically with a velocity twice that of the shadow edge and Kikuchi pattern, which move as a whole as if they were fixed to the crystal. During the rotation, therefore, the spot  $S$  crosses various Kikuchi lines successively. The conditions that  $S$  comes at the points  $A$  and  $B$  on the horizontal Kikuchi lines 440 and 660 in Fig. 2 imply that the incident electrons satisfy the Bragg conditions on 440 and 660, respectively. The condition under which  $S$  comes at the point  $C$  on the oblique Kikuchi line 351 corresponds to the Bragg condition

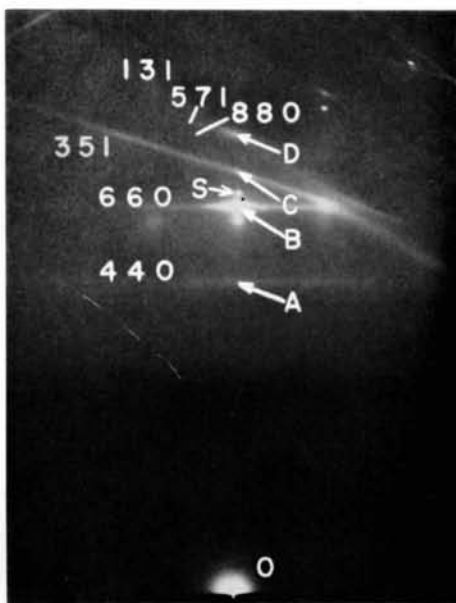


Fig. 2. Diffraction pattern from a cleavage face (110) of zincblende, for the azimuth deviating about  $5^\circ$  from the  $[\bar{1}12]$  zone axis. *O*: direct spot, *S*: specular spot, *hkl*: indices of Kikuchi lines. Meanings of *A*, *B*, *C* and *D* are explained in the text. 30 keV.

on  $35\bar{1}$ , as was previously pointed out (Miyake, Kohra & Takagi, 1954).\* The point *D*, where a horizontal and two oblique Kikuchi lines cross, nearly corresponds to the condition for the simultaneous reflexions of  $880$ ,  $13\bar{1}$  and  $57\bar{1}$ .

Pattern observations were made before and after, and also during, each run of the X-ray intensity measurements, either visually or by taking photographs.

### Results

Fig. 3 is an example of measurements obtained in the earliest stage of the study, showing the intensity variation of Zn  $K\alpha$  emission observed as a function of the glancing angle  $\alpha$ . The crystal azimuth concerned is the same as that for the diffraction pattern in Fig. 2. The ordinate is on an arbitrary scale. Anomalous dips in intensity are clearly seen in it at the positions *B*, *C* and *D*. The intensity decrease accompanying each dip is about 15 to 20% of the total intensity for *C* and *D*, while it is less remarkable for *B*.

It is noted that the curve of Fig. 3 is accompanied by a general inclination besides the anomalous dips. However, such inclination was found to depend sensitively on the geometrical condition of the incident electron beam relative to the crystal surface. In fact, the curves obtained showed sometimes even the opposite inclination. If the total flux of electron beam impinging on the surface could be kept constant during the crystal rotation, the curve would be without inclination, even though an intensity decrease at too small glancing angles will be unavoidable. The ideal geometrical condition may be prepared if the electron beam is fine enough and the crystal is perfectly set so that the rotating axis passes exactly through the crystal surface. Otherwise, the electron flux striking the crystal surface will change during the rotation of crystal as a result of, say, the straying of a part of the electron beam from the surface.

In practice, it was rather difficult to ensure the ideal condition in every case, especially in measurements over a wide range of  $\alpha$ , owing to small values of the glancing angle being of the order of  $1^\circ$ – $4^\circ$ , and to the difficulty of setting the crystal precisely. For a limited range of  $\alpha$ , however, intensity curves which are fairly reproducible except for the absolute values could be obtained as shown below.

Fig. 4 is another example of the intensity curve for the same crystal azimuth as in Fig. 2, obtained with a larger amplification of the recording system. Fig. 5 shows a comparison of the results of three independent measurements for the same azimuth, in which the ordinate is normalized at a point on the right side of each curve. Curve (*b*) is a transcription of that shown in Fig. 4. Although there are some differences in fea-

\* Since the plane (110) parallel to the crystal surface is a symmetry plane, the Kikuchi line  $35\bar{1}$  should pass the direct spot, *O*, at the condition under consideration, and this is the very condition for Bragg reflexion  $35\bar{1}$ .

tures over the whole angular range between the three curves, one may see that the main feature of the profile of each dip is almost reproducible. It is thus evident that the intensity profile about each dip is accompanied by such an asymmetry that the intensity at the shoulder on the low-angle side is weaker for dips *C* and *D*, and stronger for dip *B*, than on the high-angle side.

Fig. 6 shows two examples of the intensity curves for region *A* corresponding to the Bragg condition on  $440$ . There is an experimental difficulty because this range has the smallest glancing angles, where the beam condition relative to the crystal surface is most sensitive to the crystal setting. The sudden intensity decrease at a low angle indicated by the arrow *f* in Fig. 6(*b*), for instance, is no doubt to be ascribed to the circumstance that a part of the electron beam has begun here to stray from the crystal surface with the decreasing glancing angle. It is very likely that the intensity curves would run in the way shown by the dotted curves if a constant beam condition were kept down to lower angles. Judging from the trend of the curves, thus, it is almost certain that the X-ray intensity about the dip *A* is stronger at the shoulder on the low-angle side.

### Theory

#### General considerations

By excitation of fast electrons, a crystal may emit, as mentioned already, continuous X-rays due to the 'bremsung' and characteristic X-rays due to the ionization of electron shells in atoms. For excitation of X-rays, electrons inelastically scattered in the crystal are also responsible. However, the following considerations concern only the characteristic X-rays excited by electrons with the primary energy, because only this part of the X-rays is expected to depend on the diffraction condition of electrons.

On the basis of the treatment of Hirsch *et al.* (1962), Hall (1966) gave a theory on the emission yield of characteristic X-rays by considering that the ionization probability of an electron shell is proportional to the

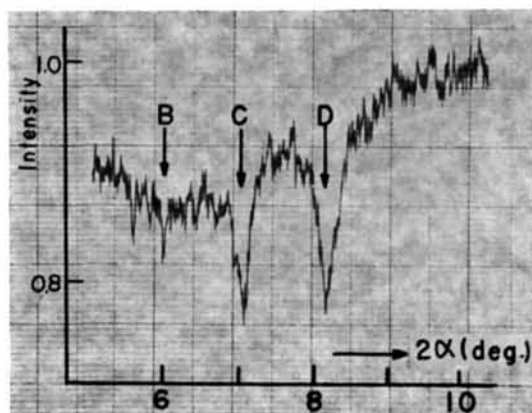


Fig. 4. Intensity curve for the same azimuth as in Fig. 2, with a higher amplification. 30 keV.

part due to this shell of the total cross section of inelastic electron scattering. The differential cross section for the inelastic scattering by, say, the  $K$  shell, is given in terms of the following matrix element

$$M_{0n}^j = \int_{\Omega} b_{[n]}^* \left[ \int \varphi_n^* \frac{e^2}{|r-r_K|} \varphi_0 dr_K \right] b^j dr \quad (1)$$

where  $r$  and  $r_K$  are the position vectors of the flying electron and of the  $K$ -shell electron, respectively,  $\varphi_0$  and  $\varphi_n$  are the wave functions for the ground state and the  $n$ th excited states of a  $K$ -shell electron in an atom, respectively, and  $b^j$  and  $b_{[n]}$  are the Bloch functions for a flying electron before and after the scattering, respectively;  $\Omega$  is the atomic volume and  $j$  is the index specifying a tiepoint on the dispersion surface in reciprocal space. Hall put  $b^j$  in the form of the two-wave approximation

$$b^j = c_0^j \exp(2\pi i k_0^j \cdot r) + c_g^j \exp(2\pi i k_g^j \cdot r), \quad (2)$$

where  $k_g^j = k_0^j + g$ ,  $g$  being a reciprocal lattice vector, while the inelastically scattered wave  $b_{[n]}$  was assumed to be a plane wave of the form  $\exp(2\pi i k_{[n]} \cdot r)$ . Although  $b_{[n]}$  should also be a Bloch wave in general, the plane wave approximation seems to be justifiable because the scattered wave is subject to Bragg conditions only accidentally. By use of the mathematical relation (Bethe, 1930)

$$\int \frac{e^2}{|r-r_K|} \exp[-2\pi i S \cdot r] dr = \frac{e^2}{\pi S^2} \exp[-2\pi i S \cdot r_K] \quad (3)$$

he obtained the equation

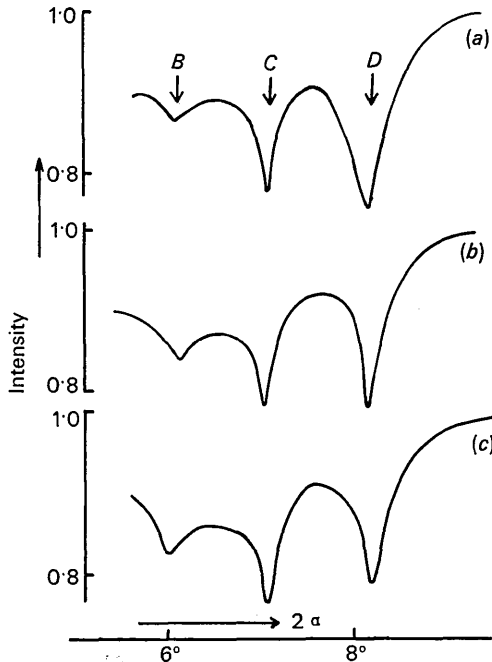


Fig. 5. Comparison of three independent measurements for the azimuth corresponding to Fig. 2. 30 keV.

$$M_{0n}^j = \frac{1}{\pi} \left\{ c_0^j \frac{D_{0n}(S_{[n]})}{|S_{[n]}|^2} + c_g^j \frac{D_{0n}(S_{[n]}-g)}{|S_{[n]}-g|^2} \right\}, \quad (4)$$

where

$$S_{[n]} = k_{[n]} - k_0^j \quad (5)$$

$$D_{0n}(S) = \int_{\Omega} \varphi_n^*(r_K) \exp[-2\pi i S \cdot r_K] \varphi_0(r_K) dr_K. \quad (6)$$

The present experiment may also be discussed along the line of Hall's considerations quoted above. There are, however, some important differences between our case and his. His theory concerns the Laue case for a thin crystal corresponding to his transmission experiment, and therefore the wave vectors  $k_g^j$  as well as  $k_0^j$  are always real so long as the absorption of electrons is disregarded. Although these vectors will become complex in an absorbing crystal, the neglect of the absorption is not very serious for a thin crystal.

The present case, on the other hand, concerns the Bragg case for a crystal with infinite thickness, so that the wave vectors become complex in the range of Bragg condition even for a non-absorbing crystal. It is to be noticed that equation (3) does not hold when  $S$  is complex.

In the present case, moreover, it is absolutely necessary to take account of the absorption effect of electrons, because the number of X-ray photons emitted in unit time from a semi-infinite and transparent crystal must turn out to be infinite. Thus, the problem one has to deal with here is the Bragg case for an absorbing crystal, in which it is very essential that the wave vectors are complex under every condition, not only in the neighbourhood of Bragg condition.

We, therefore, put

$$k_0^j = k_0^{j,r} + iq^j z \quad (7)$$

where  $k_0^{j,r}$  represents the real part of vector  $k_0^j$ , and  $iq^j z$ , the imaginary part;  $z$  is a unit vector in the direction of the inward normal to the crystal surface. With (2) and (7), the matrix element (1) concerning the  $l$ th atom in the crystal may, then, be approximated by

$$M_{0n}^{j(l)} = \exp[-2\pi q^j z_l] \cdot \int_{\Omega} \exp(-2\pi i k_{[n]} \cdot r) \cdot \left[ \int \varphi_n^* \frac{e^2}{|r_K-r|} \varphi_0 dr_K \right] \times [c_0^j \exp(2\pi i k_0^{j,r} \cdot r) + c_g^j \exp(2\pi i k_g^{j,r} \cdot r)] dr, \quad (8)$$

where  $z_l$  is the depth of the atom concerned from the surface, and  $k_g^{j,r}$  is the real part of  $k_g^j$ . \* Using relation (3) the square of the absolute value of  $M_{0n}^{j(l)}$  is calculated to be

$$|M_{0n}^{j(l)}|^2 = \frac{1}{\pi} \exp[-4\pi q^j z_l] \left\{ |c_0^j|^2 \frac{|D_{0n}(S_{[n]})|^2}{|S_{[n]}|^4} + \right.$$

\* To be more strict, an imaginary component of  $k_{[n]}$  should also be taken into account in an absorbing crystal. This circumstance is neglected, however.

$$|c_g^j|^2 \frac{|D_{0n}(S_{[n]}^{j,r} - \mathbf{g})|^2}{|S_{[n]}^{j,r} - \mathbf{g}|^4} + \frac{c_0^j c_g^j * D_{0n}(S_{[n]}^{j,r}) D_{n0}(S_{[n]}^{j,r} - \mathbf{g}) + c_0^j * c_g^j D_{n0}(S_{[n]}^{j,r}) D_{0n}(S_{[n]}^{j,r} - \mathbf{g})}{|S_{[n]}^{j,r}|^2 |S_{[n]}^{j,r} - \mathbf{g}|^2} \Bigg\}, \quad (9)$$

where  $S_{[n]}^{j,r}$  is the real part of the scattering vector defined by (5).

The total cross section for the inelastic scattering of each  $K$  shell is proportional to the integral of  $|M_{0n}^{j,(D)}|^2$  over the direction of  $\mathbf{k}_{[n]}$ , and that of the crystal as a whole is given by the sum of such integrals over atoms in crystal. The last mentioned summation may be replaced by an integration. Finally, the emission yield of  $K$  radiation,  $P_K^j$ , or the number of X-ray photons emitted in unit time from the crystal, is expressed in the form

$$\frac{P_K^j}{I_0} = A \cdot n \frac{1}{\sin \alpha} \frac{1}{2q^j} \{ p_{K,0}^j (|c_0^j|^2 + |c_g^j|^2) + 2p_{K,g}^j \cdot \text{Re} \cdot c_0^j c_g^j \}, \quad (10)$$

where  $D_{0n}$  has been assumed to be real, and  $I_0$  is the total flux of incident electron beam impinging on the crystal surface,  $A$  is a constant,  $n$  is the number of atoms under consideration in unit volume,  $\alpha$  is the glancing angle, and  $\text{Re}$  specifies the real part;  $p_{K,0}^j$  and  $p_{K,g}^j$  are defined as

$$p_{K,0}^j = \int \frac{k_{[n]}}{k_0} \cdot \frac{|D_{0n}(S_{[n]}^{j,r})|^2}{|S_{[n]}^{j,r}|^4} dS_{[n]} \quad (11a)$$

$$p_{K,g}^j = \int \frac{k_{[n]}}{k_0} \cdot \frac{D_{0n}(S_{[n]}^{j,r}) D_{n0}(S_{[n]}^{j,r} - \mathbf{g})}{|S_{[n]}^{j,r}|^2 \cdot |S_{[n]}^{j,r} - \mathbf{g}|^2} dS_{[n]}, \quad (11b)$$

where  $dS_{[n]}$  is the volume element in  $S_{[n]}$ -space.

Although in some general cases the sum of (10) over possible tiepoints on the dispersion surface should further be considered, this summation is not necessary so far as the two-wave approximation of the Bragg case for a thick crystal is concerned, as will be shown later. In such a case, the index  $j$  can be omitted and  $c_0$  may be put to be equal to unity, and thus equation (10) is written as

$$\frac{P_K}{I_0} = A \cdot n \frac{1}{\sin \alpha} \frac{1}{2q} \{ p_{K,0} (1 + |r|^2) + 2p_{K,g} \text{Re} \cdot r \}, \quad (12)$$

where

$$r \equiv \frac{c_g}{c_0} = c_g. \quad (13)$$

#### Application to simple cases

As known from (10), the emission yield of X-rays can be calculated in terms of  $q^j$ ,  $c_{0,g}^j$  and  $p_{K,0,g}^j$ . Of these, the quantities  $q^j$ , and  $c_{0,g}^j$  are given by solving each diffraction problem.

The absorption of electrons in crystal is taken into account by assuming a phenomenological complex potential

$$V(\mathbf{r}) = V^r(\mathbf{r}) + iV'(\mathbf{r}), \quad (14)$$

where  $V^r(\mathbf{r})$  is the periodic potential in the crystal, and the imaginary potential  $iV'(\mathbf{r})$  is responsible for the absorption. Let us put

$$\frac{2me}{\hbar^2} V(\mathbf{r}) = \Sigma v_h \exp 2\pi i \mathbf{h} \cdot \mathbf{r} \quad (15)$$

$$v_h = v_h^r + i v_h' \quad (16)$$

where  $\mathbf{h}$  is a reciprocal lattice vector, and  $v_h^r$  and  $v_h'$  correspond to Fourier terms of  $V^r(\mathbf{r})$  and  $V'(\mathbf{r})$ , respectively. For the Bloch wave of the form  $b = \Sigma c_h \exp(2\pi i \mathbf{k}_h \cdot \mathbf{r})$ , the well-known fundamental equations of the dynamical theory of electron diffraction (Bethe, 1928) stand as

$$(\kappa_0^2 - k_h^2) c_h + \sum_{h'} c_{h'} v_{h-h'} = 0, \quad (17)$$

where

$$\kappa_0^2 = K^2 + v_0, \quad K^2 = \frac{2me}{\hbar^2} E, \quad (18)$$

$E$  being the electron energy.

#### (i) One-wave approximation

As the most simple application, we consider a plane wave which is substantially not subject to any Bragg condition in the crystal. In this case only  $c_0$  is finite, and we obtain immediately from (17) the equation

$$k_0^2 = \kappa_0^2 \equiv K^2 + v_0^r + i v_0', \quad (19)$$

and by neglecting the second order small quantities we have

$$k_0 = (K^2 + v_0^r)^{\frac{1}{2}} + i \frac{v_0'}{2K}. \quad (20)$$

The imaginary Fourier potential  $v_0'$  is related to the mean absorption coefficient  $\mu_0$  by

$$\mu_0 = 2 \frac{2\pi v_0'}{2K} = \frac{2\pi v_0'}{K} = 2\pi \lambda v_0', \quad (21)$$

where  $\lambda$  is the wavelength of incident electrons.

Because the tangential component of  $\mathbf{k}_0$  to the crystal surface has to be equal to that of the incident wave,  $K \cos \alpha$ , the magnitude of the normal component of  $\mathbf{k}_0$ ,  $v$ , is given as

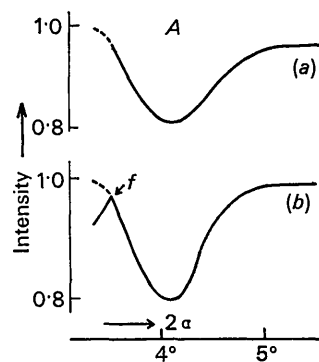


Fig. 6. Two examples of intensity curves for the range of 440 reflexion (condition  $A$ ) for the azimuth corresponding to Fig. 2. 30 keV.



$$\begin{aligned} v &= (K^2 + v_0^r + iv_0' - K^2 \cos^2 \alpha)^{\frac{1}{2}} \\ &\simeq (K^2 \sin^2 \alpha + v_0^r)^{\frac{1}{2}} + i \frac{v_0'}{2K \sin \alpha}. \end{aligned} \quad (22)$$

Therefore, the quantity  $q$  in (6) turns out to be

$$q = \frac{v_0'}{2K \sin \alpha} = \frac{\mu_0}{4\pi \sin \alpha} \quad (23)$$

and equation (12) becomes

$$\frac{P_K}{I_0} = A \cdot n \frac{2\pi}{\mu_0} p_{K,0}. \quad (24)$$

Equation (24) shows that the X-ray emission under non-Bragg conditions is independent of the glancing angle  $\alpha$ .

### (ii) Symmetrical Bragg case

As the second example, we consider a two-wave problem involving the  $g$  reflexion of the symmetrical Bragg case. Two tiepoints on the dispersion surface are determined as usual by the line  $NN'$  perpendicular to the crystal surface due to the boundary condition as schematically illustrated in Fig. 7, where  $MM'$  is the line passing through  $L$  and parallel to the crystal surface. Since the distances of the tiepoints  $A_1$  and  $A_2$  (or  $B_1$  and  $B_2$ ) from the line  $MM'$  are the same, the positions of these points relative to this line may be represented by the parameter

$$\delta = \pm \Delta,$$

where  $\Delta$  is a positive quantity, and the signs  $+$  and  $-$  apply to the points lying downwards (like  $A_1$ ) and upwards (like  $A_2$ ), respectively. If we denote the normal component of the wave vector  $\mathbf{K}$  of the incident wave by  $N$ , and consider the condition of the tangential con-

tinuity of wave vectors at the crystal boundary, then the quantities  $\kappa_0^2 - k_0^2$  and  $\kappa_0^2 - k_g^2$  in the fundamental equations (17) are given as follows (Kohra & Shinohara, 1948)

$$\kappa_0^2 - k_0^2 = (N^2 + v_0) - (|g|/2 - \delta)^2 \quad (25)$$

$$\kappa_0^2 - k_g^2 = (N^2 + v_0) - (|g|/2 + \delta)^2. \quad (26)$$

The value of  $\delta$  is determined by the secular equation

$$(\kappa_0^2 - k_0^2)(\kappa_0^2 - k_g^2) = v_g v_{-g} \quad (27)$$

and we have also the relation

$$r = \frac{c_g}{c_0} = - \frac{\kappa_0^2 - k_0^2}{v_{-g}} = - \frac{v_g}{\kappa_0^2 - k_g^2}. \quad (28)$$

Because the (110) plane of zincblende is a mirror plane, we may put  $v_h^r = v_{-h}^r$  and  $v_h' = v_{-h}'$  for  $nn0$  reflexions. Using these conditions, a straightforward calculation of (27) for an absorbing crystal determines  $\delta$  to be

$$\delta = \pm \frac{|V_g^r|}{|g|} \{ (W^2 - 1 - \sigma^2) + 2i(\sigma W - \kappa) \}^{\frac{1}{2}}, \quad (29)$$

where

$$|V_g^r| = (|v_g^r|^2 - |v_g'^2|)^{\frac{1}{2}} = |v_g^r| \cdot (1 - \kappa'^2)^{\frac{1}{2}} \quad (30)$$

$$\kappa = \frac{v_g^r v_g'}{|V_g^r|^2} = \frac{\kappa'}{(1 - \kappa'^2)}, \quad \kappa' = \frac{v_g'}{v_g^r} \quad (31)$$

$$\sigma = \frac{v_0'}{|V_g^r|} \quad (32)$$

$$\begin{aligned} W = \frac{K^2}{|V_g^r|} (\sin^2 \alpha - \sin^2 \theta_B) &\simeq \frac{2K^2}{|V_g^r|} \sin \theta_B \\ &\times (\sin \alpha - \sin \theta_B), \end{aligned} \quad (33)$$

$\theta_B$  being the Bragg angle. Parameters  $\kappa$ ,  $\kappa'$  and  $\sigma$  can be taken as positive quantities.\*

In problems of the Bragg case for a semi-infinite crystal, one of the pair of tiepoints such as  $A_1$  and  $A_2$  is to be discarded, by the criterion either that the electron flow of the permissible wave field should be directed downwards (Niehrs, 1959), or that the wave field should be one which damps with the increasing depth from the surface (Kohra *et al.*, 1948). Since the electron flow is in the direction of the normal to the dispersion surface at the relevant tiepoint, it is clear from Fig. 7 that the tiepoint to be chosen is  $A_1$  in the range (i) ( $W < -1$ ), and  $B_2$  in the range (iii) ( $W > 1$ ). As to the range (ii) ( $-1 < W < 1$ ), the second criterion may be used for due choice.

By further considerations taking account of the above circumstances, it is concluded that the signs  $+$  and  $-$  in (29) apply to the tiepoint for the  $a$  range in which  $\sigma W - \kappa < 0$ , and that for the  $b$  range in which

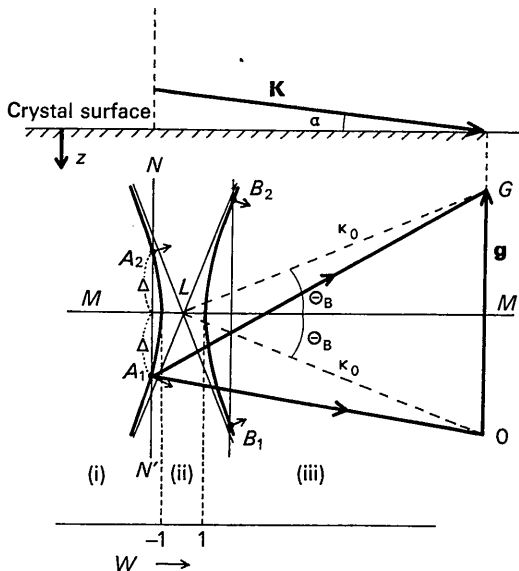


Fig. 7. Dispersion curve in reciprocal space corresponding to a symmetrical Bragg case.  $\theta_B$ : Bragg angle within the crystal.

\* As to the treatment of the symmetrical Bragg case for an absorbing crystal, refer to Zachariassen (1945), Laue (1960), James (1963), *etc.*  $W$ , which is an angle parameter corresponding to the excitation error following Bethe's notation, is essentially the similar quantity to Zachariassen's  $y$ , Laue's  $\beta'$ , James's  $p$ .

$\sigma W - \kappa > 0$ , respectively. The real part of  $\delta$ ,  $\text{Re.}\delta$ , and the imaginary part,  $\text{Im.}\delta$ , are calculated as

$$\text{Re.}\delta = \pm \frac{|V_g^2|}{|g|} \left\{ \frac{1}{2}(W^2 - 1 - \sigma^2 + [(W^2 - 1 - \sigma^2)^2 + 4(\sigma W - \kappa)^2]^{\frac{1}{2}} \right\}^{\pm} \quad (34)$$

+ for *a* range ( $\sigma W - \kappa < 0$ ), including range (i) and a part of range (ii),

– for *b* range ( $\sigma W - \kappa > 0$ ), including range (iii) and a part of range (ii);

$$\text{Im.}\delta = - \frac{|V_g^2|}{|g|} \left\{ \frac{1}{2}(-W^2 + 1 + \sigma^2 + [(W^2 - 1 - \sigma^2)^2 + 4(\sigma W - \kappa)^2]^{\frac{1}{2}} \right\}^{\pm} \quad (35)$$

over the whole range of  $W$ .

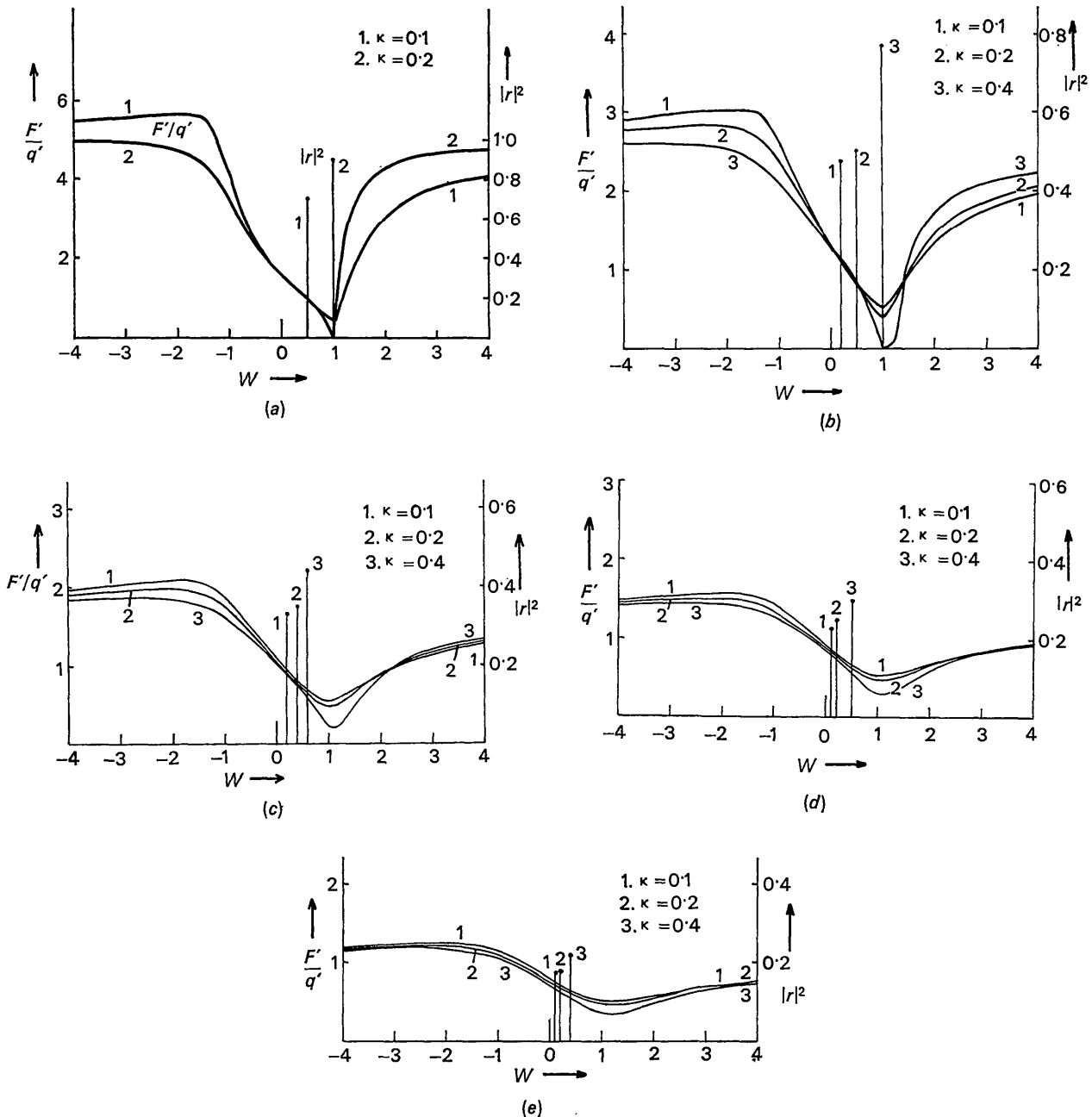


Fig. 8.  $F'/q'$  as functions of  $W$ , and the peak-positions and heights of the reflectivity curves,  $|r|^2$ , for various values of  $\sigma$  and  $\kappa$ . (a)  $\sigma=0.2$ , (b)  $\sigma=0.4$ , (c)  $\sigma=0.6$ , (d)  $\sigma=0.8$ , (e)  $\sigma=1.0$ . The values of  $\kappa$ , 0.10, 0.20, and 0.40, correspond to those of  $\kappa'$ , 0.99, 0.19, and 0.35, respectively.



By a simple consideration, the quantity  $q$  in (7) or (12) is related to  $\text{Im}.\delta$  as

$$\text{Im}.\delta = -q. \quad (36)$$

The quantity  $r = c_g/c_0$  in (12) and (13) may be calculated from relations (25), (26), (28) and (29), and is given as

$$r = \frac{c_g}{c_0} = - \frac{(1 - \kappa'^2)^{\pm}}{1 + i\kappa'} \cdot \frac{|v_g^r|}{v_g^r} \{ (W + i\sigma) \pm [(W^2 - 1 - \sigma^2) + 2i(\sigma W - \kappa)]^{\pm} \}, \quad (37)$$

where the double signs  $+$  and  $-$  correspond to the  $a$  and  $b$  regions, respectively. If we put the factor in the curly bracket in (37) as

$$- \{ \} = R + iI, \quad (38)$$

where  $R$  and  $I$  are real quantities, we obtain

$$-R = W \pm \left\{ \frac{1}{2}(W^2 - 1 - \sigma^2) + [(W^2 - 1 - \sigma^2)^2 + 4(\sigma W - \kappa)^2]^{\pm} \right\}^{\pm} \quad (39)$$

+ for  $a$  range ( $\sigma W - \kappa < 0$ )

- for  $b$  range ( $\sigma W - \kappa > 0$ )

$$-I = \sigma - \left\{ \frac{1}{2}(-W^2 + 1 + \sigma^2) + [(W^2 - 1 - \sigma^2)^2 + 4(\sigma W - \kappa)^2]^{\pm} \right\}^{\pm} \quad (40)$$

over the whole range of  $W$ .

The square of the absolute value of  $r$ ,  $|r|^2$ , is the reflectivity of electrons by the crystal surface, and is calculated to be

$$|r|^2 = \frac{1 - \kappa'^2}{1 + \kappa'^2} \cdot (R^2 + I^2). \quad (41)$$

The real part  $\text{Re}.r$  is given from (37) and (38) as

$$\text{Re}.r = \frac{(1 - \kappa'^2)^{\pm}}{1 + \kappa'^2} \cdot \frac{|v_g^r|}{v_g^r} \cdot (R + \kappa'I) \quad (42)$$

and equation (12) can be expressed in the form

$$\frac{P_K}{I_0} = A \cdot n \cdot \frac{1}{\sin \alpha} \cdot p_{K,0} \cdot 2q \cdot F(W, p_{K,g}/p_{K,0}, \kappa', \sigma) \quad (43a)$$

$$F_K = \left\{ 1 + \frac{1}{1 + \kappa'^2} \left[ (1 - \kappa'^2)(R^2 + I^2) + 2 \frac{p_{K,g}}{p_{K,0}} \frac{|v_g^r|}{v_g^r} (1 - \kappa'^2)^{\pm} (R + \kappa'I) \right] \right\} \quad (43b)$$

where we may put  $|v_g^r|/v_g^r = 1$ .\*

In order to see the general behaviour of  $P_K$ , the value of  $F/q'$  in (43) was calculated as function of  $W$

\* The phase of  $|v_g^r|/v_g^r$ , and accordingly that of  $\text{Re}.r$ , depends on the position of the coordinate origin that is to be assumed on the boundary surface. However, the quantity  $p_{K,g} \cdot |v_g^r|/v_g^r$  can be proved to be invariant. If the origin is located at the centre of an atom lying on the top layer of atoms, we have  $|v_g^r|/v_g^r = +1$ , and we may assume the sign of  $p_{K,g}$  be  $+$ . It is of course more reasonable to assume the crystal boundary at a mid-plane between adjacent atomic planes, but the result does not change.

for several combinations of the parameter  $\sigma$  and  $\kappa \equiv \kappa'/(1 - \kappa'^2)$ , where  $q'$  represents  $q$  without the factor  $|V_g^r|/|g|$  in it [see (35) and (36)]. In this calculation, however, the unknown quantities  $p_{K,0}$  and  $p_{K,g}$  were assumed to satisfy  $p_{K,0} = p_{K,g}$ , corresponding to a point scatterer being responsible for the inelastic electron scattering (Hirsch *et al.*, 1962; Hall, 1966). Further, for simplicity,  $F$  was replaced by the approximated form

$$F = 1 + (R^2 + I^2) + 2(R + \kappa'I) \quad (44)$$

which is valid for small values of  $\kappa'$ . Some examples of the results are shown in Fig. 8. A vertical bar in these figures, and the top of each bar, mark the peak position and peak height, respectively, of the relevant reflectivity curve corresponding to  $|r|^2$  given by (41).

Incidentally, it can be proved that the value of  $q$  given by (35) and (36) tends to

$$q \rightarrow \frac{|V_g^r|}{|g|} \cdot \rho = \frac{2K \sin \theta_B}{v_0}$$

when  $|W| \rightarrow \infty$ , in conformity with equation (23).

## Discussion

Theoretical calculations shown by the examples of Fig. 8 indicate that the X-ray emission yield is accompanied by a dip with an asymmetric profile in the region of each Bragg condition. It is expected that the X-ray intensity is proportional, first of all, to the penetration depth of the primary electrons below the crystal surface. Since this depth may be represented by the factor  $1/2q$  in equation (12), the intensity dip is a natural consequence of a sudden decrease of  $1/2q$  in the region of the Bragg condition, mainly due to the well-known primary extinction effect.

One of the features of the asymmetry predicted by theory is that the X-ray intensity at the shoulder corresponding to the low-angle side of the dip is stronger than at the high-angle side. As is widely known, the wave field of electrons within the crystal makes nodal planes which coincide with the atomic planes responsible for Bragg reflexion, when the glancing angle is on the low-angle side near  $W \simeq -1$  [region (i)], and anti-nodal planes, when the glancing angle is on the high-angle side near  $W \simeq 1$  [region (iii)]. In the former region, the absorption is larger because of stronger interactions, so that the penetration depth, or  $1/2q$ , is small compared with that in the latter region, as shown in Fig. 9, in which the quantities  $1/q'$ ,  $F'/q'$  and the reflectivity  $|r|^2$  are drawn together for  $\sigma = 0.4$  and  $\kappa = 0.2$ . The fact that the calculated curve of  $F'/q'$  shows, as seen in Fig. 9, the opposite trend to that of  $1/q'$  implies that relatively small values of  $1/q$  in region (i) are covered by relatively large values of  $F$ , which represents the cross section for X-ray emission of each atom under a given diffraction condition.

The present study on X-ray emission by electron excitation, and Batterman's study (1962, 1964) on X-ray emission by X-ray excitation, are concerned in

common with the Bragg case. As is well known, the asymmetry of the intensity anomaly with respect to  $W$  takes place oppositely in these two cases owing to the different natures of X-ray and electron waves. The absorption of emitted X-rays within the crystal had to be taken into account in Batterman's work, but it can be disregarded in the present case because of the extremely small penetration depth of electrons. Besides these differences, there is another important difference between the two cases, as follows.

In Batterman's study, the cross section of X-ray excitation is essentially the same as that for the X-ray absorption.\* In the case considered by us, on the other hand, the cross section for X-ray emission is substantially different from that for the absorption of electron waves in the crystal, although the former contributes to the latter very slightly. It is for this reason that in Batterman's study the profile of the anomalous dip takes nearly a complementary shape of the reflectivity curve, while in the present case it is not so, as seen in Fig. 9.

Since the theory dealt with in the foregoing section is for the symmetrical Bragg case, the calculated results may be compared with the experimental curves for the regions  $A$  and  $B$  corresponding to the Bragg conditions on 440 and 660, respectively. The experimental curves in Figs. 3-6 are in qualitative agreement with theoretical prediction with respect to the asymmetry of the profiles about the dips  $A$  and  $B$ .

Another characteristic of the asymmetric profile of each dip theoretically predicted is that the angular position of the minimum of dip in an X-ray emission curve does not coincide with that of the maximum of the relevant reflectivity curve, the former being in general located at a higher angle. This point, however, has not yet been confirmed experimentally, because at the present stage of experiment the simultaneous measurement of the reflectivity curve has still not yet been done.

As to the intensity profiles for the regions  $C$  and  $D$  shown in Figs. 3-5, the accompanying asymmetry is opposite to that for  $A$  and  $B$ . However, the theoretical result of the foregoing section cannot apply to regions  $C$  and  $D$  corresponding to non-asymmetrical diffraction conditions. Further, it should be pointed out that the diffraction conditions for  $C$  and  $D$  belong to considerably involved cases, as explained below.

As was first observed by Kikuchi & Nakagawa (1933), the specular spot shows a remarkable intensity

\* Batterman's discussion (1964) was made on the assumption that the energy loss (or true absorption) of X-rays in the crystal layer at the depth between  $z$  and  $z + dz$  is proportional to  $(1 - R^2) \cdot \mu_z(\zeta) \exp[-\mu_z(\zeta)z] dz$  [where  $R$ ,  $\zeta$  and  $\mu_z(\zeta)$  in his notation correspond to  $r$ ,  $W$  and  $4\pi q$  respectively in ours], by considering that the energy loss is proportional to  $\mu_z(\zeta)$ , and that the X-ray energy reaching a depth  $z$  is proportional to  $(1 - R^2) \exp[-\mu_z(\zeta)z]$ . However, it is to be noticed that the whole part of  $\mu_z(\zeta)$  does not contribute to the true absorption, and further, X-ray energy can enter into the crystal to the depth of the extinction distance even if  $(1 - R^2) = 0$  for a non-absorbing crystal. Justification of his assumption, therefore, should be given along a different approach.

enhancement when it coincides with an oblique Kikuchi line, e.g. as at the condition  $C$ . Miyake *et al.* (1954) took notice the fact that the Bragg reflexion excited under such a condition, say  $35\bar{1}$  for  $C$ , takes place almost parallel to the crystal surface, and considerations taking account of this peculiarity could give a qualitative explanation of the intensity enhancement of specular spot. Later, Kohra, Molière, Nakano & Ariyama (1962) made a more elaborate treatment of the same phenomenon, and pointed out that the analysis of this phenomenon requires inevitably a many-wave problem. Such complexity should be more serious for the region  $D$  corresponding to the cross point of a horizontal and two oblique Kikuchi lines. In view of these circumstances, theoretical considerations of the intensity profiles for  $C$  and  $D$  have to be postponed to future studies.

In this connexion, however, the following experimental facts will be worth mentioning. As was reported previously by one of the authors (Miyake, 1962), an intensity enhancement of an electron diffraction pattern as a whole, containing Kikuchi lines and bands and thermal diffuse spots, takes place at the same condition of the intensity enhancement of specular spot. Takagi (1958) pointed out that such an over-all intensity enhancement takes place asymmetrically with respect to the position of the specular spot relative to the oblique Kikuchi line concerned. No doubt, the phenomenon of over-all intensity enhancement of pattern is caused by the generation of an intense wave field in the crystal at the diffraction condition concerned. Thus, a more exact treatment of the diffraction problem in each case will give a common basis for interpreting not only the anomalous change of the X-ray emission yield, but also other interaction effects such as the phenomenon of the over-all intensity enhancement.

The X-ray intensity observed in the present experiments includes a large part of the background addi-

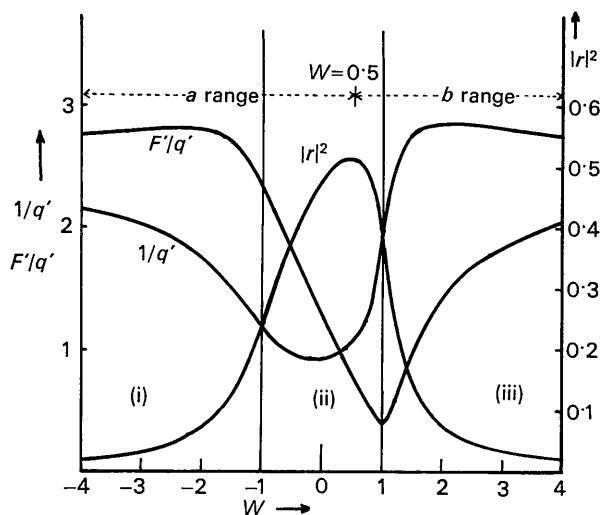


Fig. 9.  $F'/q'$ ,  $1/q'$  and  $|r|^2$  as functions of  $W$ , for  $\sigma = 0.4$ ,  $\kappa = 0.2$ .

tional to the part excited by electrons with the primary energy. This situation is more severe than in the case of the transmission experiment of Hall (1966). Under the experimental conditions of the Bragg case with a thick crystal, multiple processes of inelastic electron scattering continue until electrons wholly lose their energy in the crystal, and the integration of X-rays excited in the course of these processes inevitably makes a high background. In the case of a transmission experiment, on the other hand, the multiple process ceases when electrons emerge from a crystal which is very thin. As has already been pointed out, it should be profitable to use incident electrons of lower energies, say 10–20 keV, for the purpose of the present study. However, some other experimental difficulties will then arise.

#### References

- ANNAKA, S. (1967). *J. Phys. Soc. Japan*, **23**, 372.  
 ANNAKA, S., KIKUTA, S. & KOHRA, K. (1966). *J. Phys. Soc. Japan*, **21**, 1559.  
 BATTERMAN, B. W. (1962). *Appl. Phys. Letters*, **1**, 68.  
 BATTERMAN, B. W. (1964). *Phys. Rev.* **133**, A 759.  
 BETHE, H. (1928). *Ann. Phys. Lpz.* **87**, 55.  
 BETHE, H. (1930). *Ann. Phys. Lpz.* **5**, 225.  
 DARWIN, C. G. (1914). *Phil. Mag.* **27**, 325, 675.  
 DUNCUMB, P. (1962). *Phil. Mag.* **7**, 2101.  
 EWALD, P. P. (1917). *Ann. Phys. Lpz.* **54**, 519, 577.  
 HALL, C. R. (1966). *Proc. Roy. Soc.* **295**, 140.  
 HIRSCH, P. B., HOWIE, A. & WHELAN, M. J. (1962). *Phil. Mag.* **7**, 2095.  
 JAMES, R. W. (1963). *Solid State Physics* (Edited by Seitz & Turnbull), **15**, 55.  
 KIKUCHI, K. & NAKAGAWA, S. (1933). *Sci. Pap. Inst. Phys. Chem. Res. Tokyo*, **21**, 256.  
 KNOWLES, J. W. (1956). *Acta Cryst.* **9**, 61.  
 KOHRA, K. & SHINOHARA, K. (1948). *J. Phys. Soc. Japan*, **4**, 155, 160.  
 KOHRA, K., MOLIÈRE, NAKANO, S. & ARIYAMA, M. (1962). *J. Phys. Soc. Japan*, **17**, Suppl. B-II, 82.  
 LAUE, M. (1960). *Röntgenstrahlinterferenzen*, 3rd edition. Akademische Verlag: Frankfurt a.M.  
 MIYAKE, S., HAYAKAWA, K. & MIIDA, R. (1966). *J. Phys. Soc. Japan*, **22**, 670.  
 MIYAKE, S., KOHRA, K. & TAKAGI, M. (1954). *Acta Cryst.* **7**, 393.  
 MIYAKE, S. (1962). *J. Phys. Soc. Japan*, **17**, 1642.  
 NIEHRS, H. (1959). *Z. Phys.* **156**, 446.  
 TAKAGI, S. (1958). *J. Phys. Soc. Japan*, **13**, 287.  
 ZACHARIASEN, W. H. (1945). *Theory of X-ray Diffraction in Crystals*. New York: John Wiley.

*Acta Cryst.* (1968). A**24**, 191

## Multiple Diffraction Origin of Low Energy Electron Diffraction Intensities\*

BY A. GERVAIS, R. M. STERN AND M. MENES

*Department of Physics, Polytechnic Institute of Brooklyn, Brooklyn, N.Y., U.S.A.*

(Received 9 June 1967)

The angular and voltage dependence of the diffracted intensity for electrons in the energy range of 150–900 volts from a clean tungsten (110) surface has been measured with a single-crystal diffractometer. Selecting the angle of incidence and the electron wavelength to satisfy the Bragg condition the crystal is rotated about its normal, and a Renninger plot of diffracted intensity *versus* azimuthal angle is made. Strong intensity variations are observed when the plane of diffraction is parallel to those low index crystallographic planes which contain relatively dense atomic rows. Additional structure occurs for each intersection of an extended reciprocal lattice point with the Ewald sphere. For some orientations the intensity is reduced to half the value within one degree, which is the beam divergence. When simultaneous diffraction does not occur, the intensities of the Bragg maxima are close to the background. The integral order Bragg maxima observed in electron diffraction are thus shown to have their origin in multiple diffraction. The frequently observed fractional order Bragg maxima are predicted to have the same origin. Renninger plots for such maxima show this to be the case. In addition the appearance of the fractional order peaks should depend only on the geometry for multiple diffraction. Intensity *versus* voltage curves for the beam incident along the  $[hkl]$  direction are predicted to have maxima of order  $(h^2 + k^2 + l^2)^{-1}$ , which is verified. The implication of these observations in terms of previous two-beam models is discussed.

### Introduction

Much interest has recently been shown in obtaining a suitable theory for the diffraction of low energy electrons by single crystals. The solution of a model con-

taining the formalism for all dynamic interactions possible is quite forbidding and it is necessary to decide, in advance, which processes must be included in a theory which is expected to allow a quantitative interpretation of diffracted intensities. An examination of the literature of electron diffraction will show that there is little agreement as to the importance of dynamical

\* Supported by AFOSR Contract AF 49 (638)-1369.